DALTON
FULL PAPER

Kinetics and mechanism of the oxidation of sulfur(IV) by iron(III) at metal ion excess †

Gábor Lente and István Fábián*

University of Debrecen, Department of Inorganic and Analytical Chemistry, 4010 Debrecen, P.O.B. 21, Hungary

Received 10th August 2001, Accepted 9th October 2001
First published as an Advance Article on the web 17th January 2002

The kinetics and mechanism of the reaction between iron(III) and sulfur(IV) was studied at high iron(III) excess at 10.0 and 25.0 °C in 1.0 M $NaClO_4$ by the stopped-flow method. The number of absorbing species in this system was determined by matrix rank analysis of time-resolved spectra. The reaction exhibits composite kinetic features which could be explained by considering the reactions of $Fe(H_2O)_6^{3+}$, $Fe(H_2O)_5OH^{2+}$, $Fe_2(OH)_2(H_2O)_8^{4+}$ and two sulfito complexes, $FeSO_3(H_2O)_5^{+}$ and $Fe_2(\mu\text{-}SO_3)(\mu\text{-}OH)(H_2O)_8^{3+}$. In contrast to previous observations at sulfur(IV) excess, it was found that the kinetic traces are not influenced by the presence or absence of molecular oxygen. A detailed, ten-step kinetic model was proposed for the interpretation of the experimental observations at 340 and 430 nm. The model was validated by simultaneously fitting kinetic traces recorded at various initial concentrations to the corresponding differential equation system. It was confirmed that the dinuclear sulfito complex is not involved directly in the redox process, and the rate-determining step of the overall redox reaction is the decomposition of the mono complex in an intramolecular electron transfer step, $FeSO_3(H_2O)_5^{+}$ $(+H_2O) \longrightarrow Fe(H_2O)_6^{2+} + SO_3^{-\bullet}$. The first-order rate constant for the decomposition was determined at 10.0 and 25.0 °C to be 0.052 ± 0.012 and 0.19 ± 0.03 s^{-1}, respectively. The results imply that the sulfite ion radical is quickly oxidised to sulfate ion by iron(III) in a subsequent reaction step.

Introduction

Catalytic autoxidation of sulfur(IV) oxides has attracted considerable attention because of its dominant role in acid rain formation and industrial importance in desulfurisation of plume gases.[1–5] Recently, this reaction was also used successfully for hydroxilation, epoxidation and oxidative cleavage of DNA.[6–8] Transition metal ions are known to be very active catalysts of this oxidation process, and the stoichiometry, kinetics and mechanism of the corresponding reactions have been studied intensively since the 1930s.[1–5,9] Bäckström postulated that the formation of transition metal sulfito complexes and their decomposition are mainly responsible for the catalytic effect.[9] Since then, it has been shown that the sulfito complexes may either trigger a radical-type chain reaction by generating the $SO_3^{-\bullet}$ radical or be part of a direct oxidation of sulfur(IV) to sulfur(VI).[1] While the general features of these systems are reasonably well described and understood, important aspects are yet to be explored. Thus, the stoichiometries of the complexes formed and their exact kinetic role, as well as the pH-dependences of the individual reaction steps, need to be clarified and detailed models developed for quantitative interpretation of the kinetic phenomena.

Iron is the most abundant transition element and ferric ion-catalysed autoxidation of sulfur(IV) is the major source of acid rain formation.[1] The iron(III)–sulfur(IV) reaction holds some importance in metallurgical technologies and food chemistry as well.[10–12] Therefore, the mechanism of the catalytic reactions with various forms of iron(III) is probably one of the most extensively studied area of aqueous sulfur(IV) chemistry.[9–35] It is understood that the catalytic effect of ferric ions mostly arises from the fact that sulfur(IV) is rapidly oxidized by iron(III) and this reaction produces reactive intermediates which act as chain carriers in the autoxidation process.[30] The oxidation of iron(II) to iron(III) by molecular oxygen, which is also fast in the presence of sulfur(IV), completes the catalytic cycle efficiently.[10,28–29] In spite of the vast amount of literature data on this reaction, the conclusions reported by different authors are somewhat controversial.

In a recent study, a detailed mechanism was proposed for the iron(III)–sulfur(IV) redox reaction and the iron(III)-catalysed autoxidation of sulfur(IV).[30] The core of the reaction was identified as the fast formation and subsequent redox decomposition of sulfito complex(es). This mechanism gave a coherent interpretation of the reaction both in the presence and absence of added oxygen and was able to reproduce the specific shape of the kinetic traces, which exhibited a distinct break point when the total amount of oxygen was consumed. However, the validity of that model is limited in many ways. It does not account for the pH-dependence of the individual steps and is only applicable at pH 2.5 and large sulfur(IV) excess. The mechanism postulates the formation of a 'generalized' sulfito complex of iron(III) for which the exact composition could not be defined. The most important redox step in the overall process is the decomposition of this complex to iron(II) and sulfite ion radical ($SO_3^{-\bullet}$), but only a rough estimate could be given for its rate constant. It was concluded that the results could serve as a basis for further model development, provided that the number and exact composition of the sulfito complexes and the pH-dependences of the individual reaction steps are clarified.

In earlier and recent works, van Eldik and co-workers reported a series of $Fe(SO_3)_n^{3-2n}$ and *cis*-$Fe(SO_3)OH$ complexes.[24–27,31–33,36] In contrast, Betterton interpreted his data assuming the formation and linkage isomerisation of $Fe(SO_3)^{+}$.[34] Conklin and Hoffmann reached basically the same

† Based on the presentation given at Dalton Discussion No. 4, 10–13th January 2002, Kloster Banz, Germany.

Electronic supplementary information (ESI) available: flow scheme of stopped-flow instrument, diffusion tests, measured and fitted curves in the iron(III)–sulfite reaction and derivation of eqn. 3. See http://www.rsc.org/suppdata/dt/b1/b107263c/

 DOI: 10.1039/b107263c

conclusion on the basis of experiments carried out in a formate buffer, but did not consider the formation of formato complexes at all.[35] All of these studies used sulfur(IV) in excess over iron(III). In general, these conditions are potentially favourable for the co-existence of mono-, bis- or tris-sulfito complexes and the reactions of these species may simultaneously contribute to the experimentally observed kinetic phenomena. To avoid these complications, we designed a systematic study at high iron(III) excess which was expected to provide direct information on the formation and redox reactions of the mono-sulfito complex. However, the reaction also showed composite kinetic features under such conditions, and we confirmed the formation of two transient sulfito complexes, $FeSO_3^+$ and $Fe_2(OH)SO_3^{3+}$.[37] These results are fully supported by our related studies, which provided further evidence for the formation of a series of analogous di- and tetranuclear iron(III) complexes with simple inorganic ligands such as hypophosphite, phosphite, phosphate, arsenate and selenite ions.[38–41]

The main objective of the present work was to explore the role of these two sulfito complexes in the oxidation of sulfur(IV) by iron(III) and to develop a detailed mechanism for the interpretation of experimental observations at metal ion excess. According to our preliminary results, the complexity of this reaction prevents the use of simple data treatment methods and the experimental kinetic traces are fitted directly to a differential equation system which represents the kinetic model. Thus, the present study also provides an example of how comprehensive computation techniques can be used to evaluate composite reactive systems.

Experimental

Materials

Reagent grade Na_2SO_3 (Merck) and low chloride iron(III) perchlorate (Aldrich) were used without further purification. The iron(III) and free acid concentrations of the stock solutions were determined as described earlier.[42–43] Experiments were carried out at 10.0 ± 0.1 °C and 25.0 ± 0.1 °C. High purity $NaClO_4$ was purchased from Fluka or prepared from $HClO_4$ (Carlo Erba) and Na_2CO_3 (Reanal, Hungary) as described earlier.[44] Solutions were purged with argon to remove the dissolved oxygen, and the remaining oxygen content was determined using a YSI Model 5100 dissolved oxygen meter. It was found that the oxygen concentration of water could be routinely decreased below 0.10 mg l^{-1} from the air-equilibrated value of about 8 mg l^{-1}. Deionised and ultrafiltered water from a Millipore Q system was used for the preparation of stock solutions and samples. Sulfite ion samples were freshly prepared before use with deoxygenated water.

Instrumentation

UV-VIS spectra were recorded on an HP-8543 diode array and a UNICAM Helios-α scanning spectrophotometer. Kinetic measurements were performed with an Applied Photophysics DX-18 MV sequential stopped-flow instrument at 2 and 10 mm optical pathlengths. A standard calibration procedure gave 0.89 ± 0.04 ms for the dead time of the instrument.[45] In some cases, the kinetic traces were followed for a relatively long time in stopped-flow experiments. In these experiments, linear diffusion between the reagent or stop syringes and the optical cell could corrupt the measurements. A method to test this effect was developed and it was shown that stopped-flow curves can be used reliably up to 200 s with this instrument under the conditions applied (see ESI for details). Each kinetic curve used in the model calculations was obtained as the average of at least 5 independent runs, which were reproducible within 5%. The pH was always calculated from the composition of the samples in the kinetic runs using the appropriate equilibrium constants for the hydrolytic and protolytic reactions of iron(III) and sulfur(IV), respectively.

Computation

Non-linear least squares fitting procedures were carried out with the software package SCIENTIST.[46] Direct fitting of absorbance traces to a kinetic model was used similarly to earlier cases.[38,47–50] The kinetic model was represented by simultaneous ordinary differential equations, which were integrated using methods suitable for handling *stiff* systems with the differential equation solvers of the software packages SCIENTIST[46] and ZiTa.[51] Estimated parameters were allowed to float and the difference between the calculated and measured absorbance–time traces was minimized using non-linear least squares fitting algorithms. Parameters known independently were fixed throughout the minimizing procedure. Matrix rank analysis (MRA)[52] was carried out by calculating singular values with the software package MatLab.[53]

Results and discussion

Preliminary considerations

Typical kinetic traces recorded in the iron(III)–sulfur(IV) system indicate complex kinetic patterns at metal ion excess (Fig. 1). In

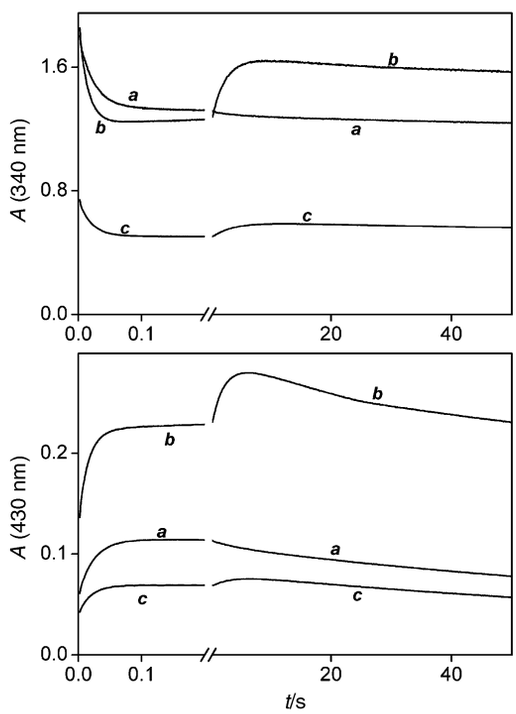

Fig. 1 Typical kinetic traces in the early phase of the iron(III)–sulfur(IV) reaction. pH = 1.40, [Fe(III)] = 25.0 mM, [S(IV)] = 0.50 mM (***a***); pH = 1.40, [Fe(III)] = 25.0 mM, [S(IV)] = 1.50 mM (***b***); pH = 1.70 [Fe(III)] = 7.5 mM, [S(IV)] = 0.50 mM (***c***); T = 10.0 °C; μ = 1.0 M ($NaClO_4$); optical pathlength 1 cm.

our earlier study, we confirmed that the initial absorbance jump and the absorbance change in the first 200 ms correspond to the formation of $FeSO_3^+$ and $Fe_2(OH)SO_3^{3+}$, respectively.[37] A sufficient interpretation could be given for the kinetic traces up to 200 ms (phase I) by considering the formation of these complexes only, and it was concluded that appreciable redox reaction does not occur in the early phase of the overall process. It was also shown that the relatively slow and pH-dependent equilibrium step between $FeOH^{2+}$ and its dimer is kinetically coupled to the iron(III)–sulfur(IV) reaction.

$$Fe_2(OH)_2^{4+} \rightleftharpoons 2FeOH^{2+} \quad (1)$$

Due to the high molar absorbance of the hydroxo dimer, the formation or consumption of this species have significant contributions to the kinetic traces even though it is always present at relatively low concentration levels. As a consequence of the slow monomer–dimer hydrolytic equilibrium, the absorbance–time profiles were markedly different depending on whether a pH-jump did or did not occur upon mixing the reactants.[37] Some of the complications could be avoided in the absence of a pH-jump, and kinetic measurements at 10.0 °C were triggered by mixing reagents of equal pH throughout this study.

Detailed kinetic analysis in this work was first carried out at 10.0 °C (λ = 340 and 430 nm). As demonstrated in Fig. 1, the system reaches a quasi-equilibrium within about 200 ms, and the corresponding reaction steps can be treated as fast pre-equilibria compared to slow hydrolytic and redox steps. On longer time scales, two not particularly well-separated phases (phase II and III) can be identified on the kinetic traces. In phase II (usually 1–10 s), the absorbance could either increase or decrease at both selected wavelengths depending on the initial concentrations. In phase III (usually >10 s) an absorbance decrease was observed at both wavelengths under all conditions. The overall reaction was not complete within 15 min at 10.0 °C. As was noted in the Experimental, stopped-flow curves cannot be evaluated reliably on such long time scales, and only the first portions of these curves were used in the calculations.

In order to verify the results obtained on the basis of the incomplete kinetic curves at 10.0 °C, the measurements were repeated at 25.0 °C. At this temperature, phase I was always complete within 50 ms and the final absorbance was reached in about 200 s. Otherwise, the kinetic curves showed the same general features at both temperatures.

Effect of oxygen

Most of the measurements at 10.0 °C were performed with oxygen-free solutions. However, in a few kinetic runs, oxygen-saturated iron(III) solutions were mixed with deoxygenated sodium sulfite ion solutions. A pair of such traces, measured at 25.0 °C, is displayed in Fig. 2 as an example. As shown, the

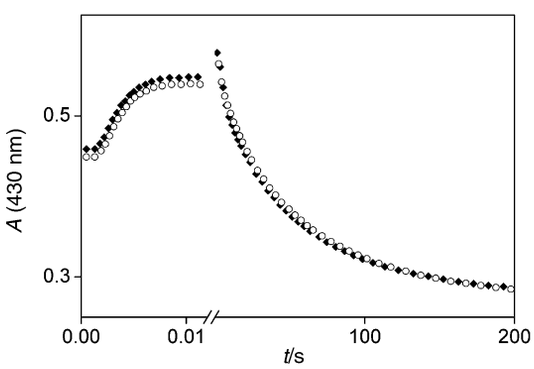

Fig. 2 Kinetic curves obtained with deoxygenated (◆) and oxygen-saturated (○) iron(III) solutions. $[Fe(III)]_0$ = 50.0 mM; $[S(IV)]_0$ = 1.00 mM; pH = 1.67; T = 25.0 °C and μ = 1.0 M ($NaClO_4$); optical pathlength 1 cm.

oxygen-free and oxygen-saturated curves are identical within experimental error. This observation indicates that oxygen may be involved in the overall reaction only after the rate-determining step under our conditions, if it is involved at all. As the presence of oxygen does not alter the kinetic traces, only the sulfite ion solutions were prepared with oxygen-free water in the experiments at 25.0 °C, in order to prevent the loss of sulfur(IV) before the kinetic runs.

At this point, it should be emphasized that oxygen is involved in a complex redox process when sulfur(IV) is used in excess and has profound effects on the kinetics of the iron(III)–sulfur(IV) reaction.[30] Thus, insufficient control over the dissolved oxygen concentration in earlier studies could be a source of uncertainty and may also be one of the reasons for the discrepancies in the literature. Our observations confirm that the artefacts due to side reactions with dissolved oxygen are completely eliminated at iron(III) excess. Accordingly, detailed studies under such conditions may provide more reliable kinetic information for the overall reaction than the experiments carried out at sulfur(IV) excess.

Spectral analysis

Single-wavelength kinetic runs are consistent with the formation of several coloured species in this system (Fig. 1). However, because of the complexity of the reaction, the identification of these species and the assignment of the spectral effects are not trivial tasks. First, in order to determine the number of dominant absorbing species, the time-resolved spectra were evaluated by MRA in the 310–450 nm spectral region.[52] In this procedure, all measured spectra are transormed into a matrix format, the singular values of this matrix are calculated and arranged in descending order. In an ideal system the number of absorbing species is given by the number of non-zero singular values. In reality, the singular values initially decrease sharply and then the differences become relatively small between the subsequent values. The slightly different small singular values are attributed to experimental error, and the number of absorbing species is given by the number of singular values in the sharply decreasing region. The singular values calculated from experimental spectra recorded at 25.0 °C are given in Table 1.

According to the MRA, there are 3 coloured species in aqueous iron(III) solutions and 5 in phase I of the iron(III)–sulfur(IV) reaction. In agreement with our earlier results, these coloured species are identified as Fe^{3+}, $FeOH^{2+}$, $Fe_2(OH)_2^{4+}$, $FeSO_3^{+}$ and $Fe_2(OH)SO_3^{3+}$. The analysis of the experimental data was repeated several times by including additional spectra recorded at gradually increasing reaction times. This procedure confirmed that the number of absorbing species remains the same during the whole reaction. Consequently, no evidence was found for the formation of new coloured species at longer reaction times, and it is reasonable to assume that any spectral change observed in the reaction is due to the transformation of the complexes formed in phase I. It follows that the absorbance increase noted in phase II is due to the accumulation of at least one of the absorbing complexes identified. The same conclusions were also valid at 10.0 °C.

Kinetics of phase II

Single wavelength kinetic traces could be fitted to double exponential functions from the end of phase I (~250 ms) up to 20–30 s at 10.0 °C. The corresponding pseudo first-order rate constants, k_{II} and k_{III}, were in agreement within the experimental error at 340 and 430 nm. At longer reaction times, the experimental kinetic traces showed significant deviations from the double exponential behaviour. It follows that only k_{II} could be assigned to a specific reaction step and used to obtain meaningful kinetic information for the overall process.

The values of k_{II} were found to be practically independent of the concentration of iron(III); however, they showed a linear dependence on the concentration of sulfur(IV). Some of the results at two different pH values are shown in Fig. 3. A comparison shows that the intercepts of the straight lines in Fig. 3 agree with the characteristic pseudo first-order rate constants for iron(III) monomer–dimer equilibration (k_{hdr}).[38,54] The corresponding values are: intercept = 0.138 ± 0.005 s^{-1}, k_{hdr} = 0.126 s^{-1} (pH = 1.40); intercept = 0.106 ± 0.011 s^{-1}, k_{hdr} = 0.109 s^{-1} (pH = 1.70). This observation suggests that phase II corresponds to the sulfite-catalysed buildup or decomposition of the dinuclear $Fe_2(OH)(SO_3)^{3+}$ complex. On the basis of

Table 1 Matrix rank analysis of spectral data in the iron(III)–sulfite ion system. 310–440 nm; 14 wavelengths; T = 25.0 °C; μ = 1.0 M ($NaClO_4$)

System	Iron(III)[a]	S(IV)[b]	S(IV)
Number of spectra	2400	3192	3992
Singular values in descending order (underlined singular values represent absorbing species).	84.4145	80.8527	110.0179
	9.5254	10.8020	11.5029
	0.6156	1.3786	1.5135
	0.0978	0.8178	1.0558
	0.0720	0.1550	0.1828
	0.0484	0.0614	0.0832
	0.0446	0.0441	0.0611
	0.0229	0.0303	0.0415
	0.0222	0.0230	0.0365
	0.0165	0.0223	0.0273
	0.0146	0.0162	0.0220
	0.0141	0.0146	0.0182
	0.0130	0.0139	0.0179
	0.0121	0.0129	0.0166
Predicted number of absorbing species	3	5	5

[a] Without sulfur(IV). [b] Only spectra recorded in the initial 50 ms were used.

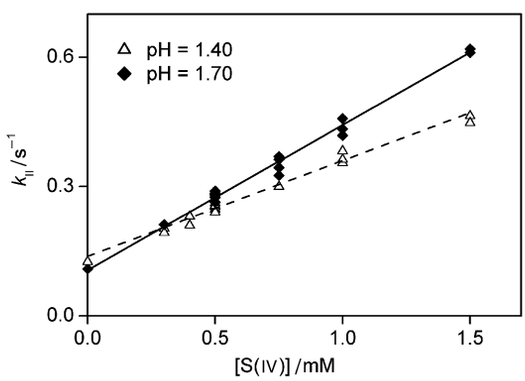

Fig. 3 k_{II} as a function of the concentration of S(IV). T = 10.0 °C; μ = 1.0 M ($NaClO_4$). Several different iron(III) concentrations were used in the range [Fe(III)] = 5.0–35.0 mM; the rate constants were found to be independent of [Fe(III)].

analogous observations in the iron(III)–sulfate ion and selenite ion systems,[40,41] the formation or decomposition of $Fe_2(OH)SO_3^{3+}$ could be responsible for the observed effect.

$$Fe_2(OH)SO_3^{3+} \rightleftharpoons FeOH^{2+} + FeSO_3^{+} \qquad (2)$$

This reaction is kinetically coupled to the dimerisation step between the monomeric and dimeric hydroxo species (eqn. 1) and the concentrations of $Fe_2(OH)(SO_3)^{3+}$ and $Fe_2(OH)_2^{4+}$, and consequently the measured absorbance, may either increase or decrease depending on the initial concentrations and pH. Provided that the protolytic equlibria of the ligand and the formation of $Fe_2(OH)(SO_3)^{3+}$ from $Fe_2(OH)_2^{4+}$ and HSO_3^- are fast pre-equilibria and the dinuclear complex is present in much smaller concentration than $Fe_2(OH)_2^{4+}$ and HSO_3^-, standard derivation yields the following expression for k_{II}:[40,41]

$$k_{II} \approx k_{hdr} + \frac{k_8 K_5 [S(IV)]}{1 + [H^+]/K_{a1}} \qquad (3)$$

(The rate and equilibrium constants in this formula are denoted as in Scheme 1.) This simplified formula does not contain the rate constant of the reverse step of eqn. 2, as its contribution to the pseudo first-order rate constant was found to be marginal (see ESI for details). All conditions, particularly a sufficiently low concentration of $Fe_2(OH)(SO_3)^{3+}$, could not always be maintained in the experiments and eqn. 3 was used only to illustrate the dominant kinetic feature of phase II and to obtain a first estimate for k_8. Because of the limitations discussed above, any attempt to give a similar interpretation for k_{III} was unsuccessful.

$$Fe^{3+} \rightleftharpoons FeOH^{2+} + H^+$$
$$K_H = [FeOH^{2+}][H^+]/[Fe^{3+}] \qquad (R1)$$

$$Fe^{3+} + HSO_3^- \rightleftharpoons FeSO_3^+ + H^+$$
$$K_F = [FeSO_3^+][H^+]/[Fe^{3+}]/[HSO_3^-] \qquad (R2)$$

$$H_2O \bullet SO_2 \rightleftharpoons HSO_3^- + H^+$$
$$K_{a1} = [HSO_3^-][H^+]/[H_2SO_3] \qquad (R3)$$

$$HSO_3^- \rightleftharpoons SO_3^{2-} + H^+$$
$$K_{a2} = [SO_3^{2-}][H^+]/[HSO_3^-] \qquad (R4)$$

$$Fe_2(OH)_2^{4+} + HSO_3^- \rightleftharpoons Fe_2(OH)SO_3^{3+}$$
$$v_5 = k_5[Fe_2(OH)_2^{4+}][HSO_3^-] - k_{-5}[Fe_2(OH)SO_3^{3+}] \qquad (R5)$$

$$Fe_2(OH)_2^{4+} + SO_3^{2-} (+ H^+) \rightleftharpoons Fe_2(OH)SO_3^{3+}$$
$$v_6 = k_6[Fe_2(OH)_2^{4+}][SO_3^{2-}] - k_{-6}[Fe_2(OH)SO_3^{3+}]/[H^+] \qquad (R6)$$

$$Fe_2(OH)_2^{4+} \rightleftharpoons 2FeOH^{2+}$$
$$v_7 = k_7[Fe_2(OH)_2^{4+}] - k_{-7}[FeOH^{2+}]^2 \qquad (R7)$$

$$Fe_2(OH)SO_3^{3+} \rightleftharpoons FeOH^{2+} + FeSO_3^+$$
$$v_8 = k_8[Fe_2(OH)SO_3^{3+}] - k_{-8}[FeOH^{2+}][FeSO_3^+] \qquad (R8)$$

$$FeSO_3^+ \rightarrow Fe^{2+} + SO_3^{-\bullet}$$
$$v_9 = k_9[FeSO_3^+] \qquad (R9)$$

$$Fe^{3+} + SO_3^{-\bullet} + H_2O \rightarrow Fe^{2+} + SO_4^{2-} + 2H^+ \quad \text{fast} \qquad (R10)$$

Scheme 1 Kinetic model for the iron(III)–sulfur(IV) reaction at iron(III) excess.

Kinetic model for the overall reaction

As discussed in our earlier study[37] and in the previous sections in detail, a very reasonable interpretation can be given for phases I and II by considering only hydrolytic, ligand substitution and mononuclear–dinuclear interconversion steps. This implies that any possible redox reaction between the reactants is slow and it may noticeably affect the kinetic patterns only at

longer reaction times. The complexity and relatively high rate of the reaction prevented us from using any detection methods other than spectrophotometry and appropriate techniques are not, as yet, available for selective and quantitative monitoring of the consumption of sulfur(IV) and the formation of ferrous and sulfate ions, which are the main products. Nevertheless, our ongoing studies using the quenched stopped-flow technique provided some evidence that the rate of accumulation of iron(II) is on the same time scale as phase III.[55] Therefore, we assign the last part of the reaction to the redox process between iron(III) and sulfur(IV) and assume that the concentrations of the reactive species in this phase are controlled by the reactions which have already been identified, most of which are in fast pre-equilibria.

A vital question is how the electron transfer actually takes place between the reactants. Earlier it was assumed that it is an inner sphere redox reaction and the sulfito complex most likely undergoes a rate-determining decomposition into Fe^{2+} and $SO_3^{-\bullet}$.[30] The sulfite ion radical is a reactive intermediate which is transferred into the final products in subsequent fast reaction steps.

In accordance with the above considerations, we postulate the model shown in Scheme 1 for the overall reaction. This scheme has some distinct features when compared to other models postulated on the basis of kinetic data at low iron(III) concentration and high sulfur(IV) excess. Most importantly, we ignore the reactions of the product Fe(II) and assume that step R10 is the only sink of the $SO_3^{-\bullet}$ radical. This implies that side reactions are not competitive with the reactions of iron(III) when the metal ion is used in large excess. The insensitivity of the kinetic profiles to the presence of oxygen lends strong support to this assumption. It was confirmed earlier that the reaction of the $SO_3^{-\bullet}$ radical with molecular oxygen opens a very efficient catalytic pathway for the oxidation of sulfur(IV) at low iron(III) concentration *via* the formation of the reactive $SO_5^{-\bullet}$ radical.[30] Such a kinetic effect is absent when iron(III) is present at large concentration levels, indicating that $SO_3^{-\bullet}$ is predominantly oxidised by iron(III) in step R10.

A further difference compared to previous models is that Scheme 1 postulates only elementary steps with well-established species. The only exception is reaction R7, which was shown to proceed *via* three competing pathways, and the following pH-dependent expression was confirmed for k_7:[54]

$$k_7 = k_{7a} + k_{7b}[H^+] + k_{7c}/[H^+] \qquad (4)$$

The relevant rate laws were explored, and the kinetic and equilibrium constants were also determined for reactions R1–R8 in independent studies.[37,38,54,56–58] Therefore, Scheme 1 is expected to be suitable for quantitative evaluation of the overall reaction and to provide satisfactory interpretation of the kinetic features.

Due to strong kinetic coupling between the individual reaction steps, more specifically between R7, R8 and R9, our attempts to derive an explicit kinetic expression for phase III were unsuccessful. Thus, the validity of the model was tested by fitting kinetic traces recorded under different experimental conditions directly to a differential equation system which represents the kinetic model. The data set at 10.0 °C included 22 kinetic runs at pH = 1.40, 17 kinetic runs at pH = 1.70, and 9 kinetic runs from the pH-range 1.10–1.90. In each run, duplicate kinetic traces were measured at two different wavelengths (340 and 430 nm), and each kinetic trace contained 1000 data points, 500 in the first 200 ms and 500 more from 0.2 s to 50 s. Thus, we simultaneously fitted about 10^5 time-dependent absorbance values in the final evaluation. Rate and equilibrium constants, as well as molar absorbances known from independent studies were included with fixed values in these calculations and only rate constants k_8 and k_9 were allowed to float. The value of k_{-8} was forced to comply with $k_{-8} = k_8K_5K_H/K_7$ on the basis of microscopic reversibility. It is assumed that R9 and R10 are irreversible, though earlier the former step was postulated as reversible. The simplification can be justified by considering that [Fe(III)] ⩾ [Fe(II)] holds for all kinetic runs, therefore the backward step of R9 is negligible compared to R10. The parameters estimated on the basis of this model are given in Table 2 and the quality of the fitting is illustrated in Fig. 4.

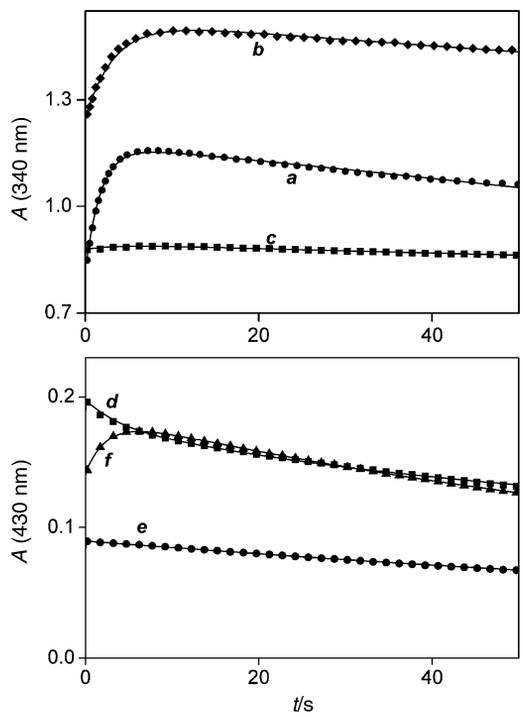

Fig. 4 Measured (marked points) and fitted (solid lines) curves in the iron(III)–sulfite ion reaction. pH = 1.40, [Fe(III)] = 20.0 mM, [S(IV)] = 0.50 mM (***a***); pH = 1.40, [Fe(III)] = 25.0 mM, [S(IV)] = 1.00 mM (***b***); pH = 1.70, [Fe(III)] = 10.0 mM, [S(IV)] = 1.50 mM (***c***); pH = 1.40, [Fe(III)] = 35.0 mM, [S(IV)] = 0.50 mM (***d***); pH = 1.40, [Fe(III)] = 20.0 mM, [S(IV)] = 0.50 mM (***e***); pH = 1.70, [Fe(III)] = 10.0 M, [S(IV)] = 1.00 mM (***f***); T = 10.0 °C; μ = 1.0 M ($NaClO_4$); optical pathlength 1 cm. Only about 7% of the measured points are shown for clarity.

In principle, the dinuclear $Fe_2(OH)SO_3^{3+}$ complex may also undergo direct redox decomposition. This possibility was tested by including the following net reaction in the model, assuming that it is initiated by a rate-determining intramolecular electron transfer from sulfur(IV) to iron(III):

$$Fe_2(OH)SO_3^{3+} + H^+ \rightleftharpoons 2Fe^{2+} + SO_4^{2-} \qquad (5)$$

However, the shape of the kinetic traces could not be reproduced when this reaction was used instead of R9, and the goodness of fit did not improve significantly when both redox steps were considered. Consequently, the rate constant of reaction 5 could not be determined with any acceptable precision and it was concluded that the contribution of this step to the overall reaction is negligible, if it occurs at all.

At 25.0 °C, the first phase of the kinetic traces was fitted as detailed in our earlier report and the whole experimental traces were evaluated using the same data treatment as at 10.0 °C. In this case, the kinetic traces contained fewer points, but the reaction was always followed until completion. The relative kinetic weights of the individual reaction steps changed somewhat with increasing temperature and, as a consequence, the reliability of certain parameters is not the same at the two temperatures. For example, only the $K_F\varepsilon$ product could be estimated for the $FeSO_3^+$ complex at 10.0 °C, while the equilibrium constant and the molar absorptivity could be separated at 25.0 °C. At the latter temperature, reaction R5 becomes dominant over R6 in

Table 2 Parameters estimated in the iron(III)–sulfur(IV) reaction. $\mu = 1.0$ M ($NaClO_4$)

Parameter	10.0 °C	25.0 °C
$\log K_H$	-3.03 [a]	-2.72 [b]
$\log K_F$	— [c]	0.13 ± 0.05
$\varepsilon\{FeSO_3^+\}$; 430 nm	— [c]	492 ± 34 M^{-1} cm^{-1}
$\log K_{a1}$	-1.49 [a]	-1.74 ± 0.01
$\log K_{a2}$	-6.44 [a]	-6.34 [d]
$\log K_5$	3.37 [a]	3.73 ± 0.11
k_5	4.5×10^4 M^{-1} s^{-1} [a]	$(3.9 \pm 0.3) \times 10^5$ M^{-1} s^{-1}
k_6	2.1×10^9 M^{-1} s^{-1} [a]	$\sim 4 \times 10^9$ M^{-1} s^{-1}
$\log K_7$	-3.08 [a]	-2.58 [b]
k_{7a}	0.059 M^{-1} s^{-1} [e]	0.35 M^{-1} s^{-1} [b]
k_{7b}	1.08 s^{-1} [e]	3.5 s^{-1} [b]
k_{7c}	5.8×10^{-4} M s^{-1} [e]	3.6×10^{-3} M s^{-1} [b]
k_8	1.0 ± 0.3 s^{-1}	3.6 ± 0.8 s^{-1}
k_9	0.052×0.012 s^{-1}	0.19 ± 0.03 s^{-1}
$\varepsilon\{Fe_2(OH)(SO_3)^{3+}\}$; 430 nm	499 M^{-1} cm^{-1} [a]	549 ± 60 M^{-1} cm^{-1}

[a] Ref. 37. [b] Ref. 54. [c] $K_F\varepsilon\{FeSO_3^+\} = 281$ M^{-1} cm^{-1} (430 nm, ref. 37). [d] Ref. 58. [e] Ref. 38. Error limits are quoted as one standard deviation only for the parameters which were determined in the present study.

the initial phase, since k_5 increases almost an order of magnitude compared to its value at 10.0 °C, whereas the change in k_6 is less than twofold and only a rough estimate can be given for its value. An analysis of the kinetic traces at 25.0 °C revealed that a simplified method could also be used for the evaluation of phase III by assuming that R5–R8 are fast pre-equilibria. In this case, only k_9 was fitted and its value was in reasonable agreement with the result obtained by comprehensive data fitting.

Conclusion

The results presented here confirm that an excellent interpretation can be given for the composite kinetic features in the iron(III)–sulfur(IV) system at metal ion excess by considering a series of coupled reactions of the well-known iron(III) hydroxo complexes and two sulfito complexes, $Fe_2(OH)SO_3^{3+}$ and $FeSO_3^+$. Under such conditions, evidence was not found for the formation of protonated, bis-, tris- or other multinuclear complexes with sulfur(IV).

It was shown that the formation of $Fe_2(OH)SO_3^{3+}$ can be considered a 'dead end' reaction because this species is not involved in direct electron transfer steps, it vanishes by the end of the reaction and is not essential for completing the redox process. In other words, a considerable portion of sulfur(IV) is coordinated in the dinuclear complex and the oxidation of sulfur(IV) would proceed even faster without the existence of this species. Nevertheless, $Fe_2(OH)SO_3^{3+}$ strongly influences the kinetics of the overall process in several ways. Thus, the substantial absorbance change in the first part of the reaction is partly due to fast formation of this species. The same process also opens a new catalytic pathway for the hydrolytic equilibrium between the mono- and dinuclear hydroxo complexes of iron(III), as the R5, R6, R8 sequence transforms these species into each other much faster than reaction R7. Finally, the concentration of the redox active $FeSO_3^+$ complex is also controlled by reaction R8 to a certain extent.

The formation of the dinuclear sulfito complex is probably not limited to the conditions used in the present study. Although $Fe_2(OH)SO_3^{3+}$ was never considered in earlier kinetic models, the reactions of this species may also prove to be significant at low iron(III) concentrations and high ligand excess when the experiments are carried out in less acidic solution. While the molar fraction of $Fe_2(OH)_2^{4+}$ decreases when the total concentration of iron(III) is decreased, the increase in pH may overcompensate this effect. In addition, sulfur(IV) is present at a relatively high concentration and the dinuclear complex may form at considerable concentration levels. It follows that rejection of the corresponding reactions is not necessarily justified and further studies are required to explore the significance of the $Fe_2(OH)SO_3^+$ complex under a wide range of experimental conditions.

According to the results, the rate-determining step of the redox reaction is the decomposition of the $FeSO_3^+$ complex. This species was postulated in earlier studies and our value for the equilibrium constant of step R2, $K_F = 1.35$, is in reasonable agreement with previous literature data, which are in the range 1.06–3.84.[25,26,34,35] Such a good agreement between these equilibrium constants is quite surprising and should be considered fortuitous when the discrepancies regarding the speciation in the iron(III)–sulfur(IV) system (*cf.* Introduction) are taken into account.

The combination of K_F and K_{a1} yields 3.0×10^6 M^{-1} for the stability constant of the mono-sulfito complex, which corresponds to the following reaction:

$$Fe^{3+} + SO_3^{2-} \rightleftharpoons FeSO_3^+ \quad (6)$$

Recently, a stable mono-sulfito complex was also reported in the mercury(II)–sulfur(IV) system which is involved in a redox decomposition very similar to that of $FeSO_3^+$.[59–60] It is reasonable to assume that a partial electron transfer from the ligand to the metal centre stabilizes the mono-complex in both cases. A complex with such an electronic structure can be regarded as an ideal precursor to the intra-molecular electron transfer step.

Perhaps the most important result of the present study is that direct kinetic information could be obtained for the intramolecular redox decomposition of the $FeSO_3^+$ complex. Reaction R9 was postulated as the key reaction step in various earlier kinetic models, but only rough estimates were reported for its rate constant. The inherent difficulty in determining this parameter is that R9 is kinetically coupled with other reaction steps and classical methods are not suitable for the evaluation of the data. Comprehensive data treatment provided a well-defined value for k_9, which is essentially the same as the value predicted by our model calculations (0.2 s^{-1} at 25.0 °C).[30]

The current results also indicate that the large number of absorbing species is the crucial barrier which must be overcome in order to explore some of the details of the overall reaction, even when non-classical evaluation methods are used. Therefore, further model developments should also rely on the use of fast kinetic methods that do not require on-line spectrophotometric detection and preferably can be used for direct determination of the concentration profiles of the reactants, products and, occasionally, the most important intermediate species. A systematic study to design such methods is under way in our laboratory.

Acknowledgements

This work was supported by the Hungarian Research Foundation under grant no. OTKA M028244 and T029568.

References

1 C. Brandt and R. van Eldik, *Chem. Rev.*, 1995, **95**, 119 and references therein.
2 A. N. Yermakov, G. A. Proskrebyshev and A. P. Purmal, *Kinet. Catal.*, 1997, **38**, 325.
3 O. A. Travina, Y. N. Kozlov, A. P. Purmal and S. O. Travin, *Kinet. Catal.*, 1997, **38**, 242.
4 H. R. Pezza, C. F. F. Lopes, M. E. V. Suárez-Iha and N. Coichev, *Quim. Nova*, 1999, **22**, 529 and references therein.
5 C. R. Martins, C. A Cabral Neto, J. J. F. Alves and J. B. de Andrade, *J. Braz. Chem. Soc.*, 1999, **10**, 453.
6 J. G. Muller, R. P. Hickerson, R. J. Perez and C. J. Burrows, *J. Am. Chem. Soc.*, 1997, **119**, 1501.
7 V. Lepentsiotis, J. Domagala, I. Grgić, R. van Eldik, J. G. Muller and C. J. Burrows, *Inorg. Chem.*, 1999, **38**, 3500.
8 K. Wietzerbin, J. G. Muller, R. A. Jameton, G. Pratviel, J. Bernadou, B. Meunier and C. J. Burrows, *Inorg. Chem.*, 1999, **38**, 4123.
9 H. L. J. Bäckström, *Z. Phys. Chem., Abt. B*, 1934, **25**, 122.
10 B. L. Tiwari, J. Kolbe and H. W. Hayden Jr., *Metall. Trans. B*, 1979, **10**, 607.
11 E. H. Cho, *Metall. Trans. B*, 1986, **17**, 745.
12 B. L. Wedziha and O. Lamikanra, *Food Chem.*, 1987, **23**, 193.
13 D. G. Karraker, *J. Phys. Chem.*, 1963, **67**, 871.
14 D. W. Carlyle, *Inorg. Chem.*, 1971, **10**, 761.
15 D. W. Carlyle and O. F. Zeck, *Inorg. Chem.*, 1973, **12**, 2978.
16 N. A. Skorik and N. A. Zatolokina, *Russ. J. Inorg. Chem.*, 1986, **31**, 1318.
17 I. Grgić, M. Poznić and M. Bizjak, *J. Atmos. Chem.*, 1990, **33**, 89.
18 O. Timpe and R. Schlögl, *Ber. Bunsen-Ges. Phys. Chem.*, 1993, **97**, 1076.
19 P. Warneck and J. Ziajka, *Ber. Bunsen-Ges. Phys. Chem.*, 1995, **99**, 59.
20 I. Grgić, A. Dovžan, G. Berčič and V. Hudnik, *J. Atmos. Chem.*, 1998, **29**, 315.
21 A. Wolf, F. Deutsch, P. Hoffmann and H. M. Ortner, *J. Atmos. Chem.*, 2000, **37**, 125.
22 A. Das and A. C. Dash, *Inorg. React. Mech.*, 2000, **2**, 101.
23 A. Das and A. C. Dash, *J. Chem. Soc., Dalton Trans.*, 2000, 1949.
24 J. Kraft and R. van Eldik, *J. Chem. Soc., Chem. Commun.*, 1989, 790.
25 J. Kraft and R. van Eldik, *Atmos. Environ.*, 1989, **23**, 2709.
26 J. Kraft and R. van Eldik, *Inorg. Chem.*, 1989, **28**, 2297.
27 J. Kraft and R. van Eldik, *Inorg. Chem.*, 1989, **28**, 2306.
28 R. van Eldik, N. Coichev, K. Bal Reddy and A. Gerhard, *Ber. Bunsen-Ges. Phys. Chem.*, 1992, **96**, 478.
29 K. Bal Reddy and R. van Eldik, *Atmos. Environ., Part A*, 1992, **26**, 661.
30 C. Brandt, I. Fábián and R. van Eldik, *Inorg. Chem.*, 1994, **33**, 687.
31 V. Lepentsiotis, F. F. Prinsloo, R. van Eldik and H. Gutberlet, *J. Chem. Soc., Dalton Trans.*, 1996, 2135.
32 F. F. Prinsloo, C. Brandt, V. Lepentsiotis, J. J. Pienaar and R. van Eldik, *Inorg. Chem.*, 1997, **36**, 119.
33 C. Brandt and R. van Eldik, *Transition Met. Chem.*, 1998, **23**, 667.
34 E. A. Betterton, *J. Atmos. Chem.*, 1993, **17**, 307.
35 M. H. Conklin and M. R. Hoffmann, *Environ. Sci. Technol.*, 1988, **22**, 899.
36 We assume that the iron(III) complexes are octahedral, and the coordinated water molecules are not given in the formulae unless they have particular significance.
37 G. Lente and I. Fábián, *Inorg. Chem.*, 1998, **37**, 4204.
38 G. Lente, M. E. A. Magalhães and I. Fábián, *Inorg. Chem.*, 2000, **39**, 1950.
39 G. Lente and I. Fábián, *React. Kinet. Catal. Lett.*, 2001, **73**, 117.
40 G. Lente and I. Fábián, *Inorg. Chem*., submitted.
41 G. Lente, Ph.D. Thesis, University of Debrecen, Hungary, 2001. Available *via* the Internet at http://www.klte.hu/~lenteg/index.html.
42 I. Fábián and G. Gordon, *Inorg. Chem.*, 1991, **30**, 3994.
43 I. Fábián and G. Gordon, *Inorg. Chem.*, 1992, **31**, 2144.
44 G. Gordon and P. Tewari, *J. Phys. Chem.*, 1966, **70**, 200.
45 B. Tonomura, H. Nakatani, M. Ohnishi, J. Yamaguchi-Ito and K. Hiromi, *Anal. Biochem.*, 1978, **84**, 370.
46 SCIENTIST, version 2.0, Micromath Software, Salt Lake City, UT, USA, 1995.
47 A. Nemes, I. Fábián and R. van Eldik, *J. Phys. Chem. A*, 2000, **104**, 7995.
48 G. Lente, J. Jacob, I. A. Guzei and J. H. Espenson, *Inorg. React. Mech.*, 2000, **2**, 169.
49 A. Nemes, I. Fábián and G. Gordon, *Inorg. React. Mech.*, 2000, **2**, 327.
50 Zs. Tóth and I. Fábián, *Inorg. Chem.*, 2000, **39**, 4608.
51 G. Peintler, ZiTa, version 4.1, Attila József University, Szeged, Hungary, 1997.
52 G. Peintler, I. Nagypál, A. Jancsó, I. R. Epstein and K. Kustin, *J. Phys. Chem. A*, 1997, **101**, 8013.
53 MatLab for Windows, version 4.2c1, The Mathworks, Inc., Natick, MA, USA, 1994.
54 G. Lente and I. Fábián, *Inorg. Chem.*, 1999, **38**, 603.
55 Zs. Hadady, G. Lente and I. Fábián, unpublished work.
56 P. Hemmess, L. D. Rich, D. L. Cole and E. M. Eyring, *J. Phys. Chem.*, 1971, **75**, 929.
57 R. H. Betts and R. H. Voss, *Can. J. Chem.*, 1970, **48**, 2035.
58 M. Frydman, G. Nilsson, T. Rengemo and L. G. Sillén, *Acta Chem. Scand.*, 1958, **12**, 878.
59 L. L. Van Loon, E. A. Mader and S. L. Scott, *J. Phys. Chem. A*, 2000, **104**, 1621.
60 L. L. Van Loon, E. A. Mader and S. L. Scott, *J. Phys. Chem. A*, 2001, **105**, 3190.